Generation of chaotic attractors using neurons with multidentrites

Salma Ben Mamia, William Puech, Kais Bouallegue

Generation of chaotic attractors using neurons with multidentrites

Salma Ben Mamia*

Electronics and Microelectronics Laboratory,
University of Monastir, Tunisia
Email: salma.ben-mamia@lirmm.fr
*Corresponding author

William Puech

LIRMM,
University of Montpellier,
CNRS, France
Email: william.puech@lirmm.fr

Kais Bouallegue

ISSAT,
Higher Institute of Applied Sciences and Technology of Sousse, Tunisia
Email: Kais bouallegue@yahoo.fr

Abstract: Compared to traditional chaotic systems like Lorenz, Chua, logistic map and Rössler systems. A different generation of new chaotic systems emerged, based on the mathematical model of a variable structure model of neurons (VSMNs). A detailed bifurcation analysis of the new chaotic system with theory and simulations is discussed. Our new discovery has some attractive features valuable for engineering applications, such as security communication. In this paper, we present some types of coupling of our new chaotic system. Using VSMN, the system can generate a single, spiral and double-scroll chaotic attractor. With changing parameters and adding oscillators, their behaviour changes into four symmetric and coexisting of double-scroll chaotic attractors. We conclude that coupling with chaotic attractors, does not only increases the chaos' complexity but also generates multi hyperchaotic attractors. Finally, we couple between two chaotic attractors using neurons, which lead to a multi-stability system. They illustrate that our multi-scroll system is hyperchaotic and its complexity can ensure a perfect security for telecommunication systems for the future.

Keywords: dendrites; hyperchaotic attractor; neural networks; variable structure model of neuron; VSMN.

Reference to this paper should be made as follows: Ben Mamia, S., Puech, W. and Bouallegue, K. (xxxx) 'Generation of chaotic attractors using neurons with multidentrites', *Int. J. Modelling, Identification and Control*, Vol. X, No. Y, pp.xxx–xxx.

Biographical notes: Salma Ben Mamia received her MS in Intelligent Systems Road Traffic Control (Hit4med) from the University of Sousse, Tunisia, in 2019. She is currently pursuing her PhD with the Laboratory of Electronics and Microelectronics in the University of Monastir, Tunisia. Her work has focused on the generation of new chaotic systems applied in image encryption by neural network.

William Puech received his Diploma of Electrical Engineering from the University of Montpellier, France in 1991 and PhD in Signal-Image-Speech from the Polytechnic National Institute of Grenoble, France in 1997 with research activities in image processing and computer vision. He served as a Visiting Research Associate to the University of Thessaloniki, Greece. From 1997 to 2008, he has been an Associate Professor at the University of Montpellier, France. Since 2009, he is a Full Professor in Image Processing at the University of Montpellier, France.

Kais Bouallegue is a Professor in the Higher Institute of Applied Sciences and Technology of Sousse, Tunisia. He received his PhD from the National Engineering School of Sfax. He is active member in different industrial companies. He has served a reviewer for technical papers. His current research interests include fractal, chaos and complex system.

1 Introduction

Chaos is a very important phenomenon in nonlinear systems which has been intensively studied in the last decades and used in many commercial applications (Ben Slimane et al., 2017; Gámez-Guzmán et al., 2009; Trejo-Guerra et al., 2009). It can be used in the encryption domain too. Benkouider et al. (2020a) created a new family of 5D, 6D, 7D and 8D hyperchaotic systems from the 4D hyperchaotic Vaidyanathan system, the dynamic analysis of the 8D hyperchaotic system with six positive Lyapunov exponents and an application to secure communication design, and an other new family of 9D and 10D hyperchaotic systems from the 8D hyperchaotic Benkouider system, the bifurcation analysis of the 10D hyperchaotic system, circuit design and an application to secure voice communication (Benkouider et al., 2020b). Ben Slimane et al. (2018b) proposed a fast and secure scheme for image encryption using the nested chaotic maps and the DNA sequence operation. They also designed an efficient image cryptosystem (Ben Slimane et al., 2018a) using a single neuron model, a chaotic map and DNA sequence operations. Puteaux and Puech (2017) put forward a new reversible data hiding method in encrypted images based on an adaptive local Shannon entropy analysis. They also suggested (Puteaux and Puech, 2018) an efficient method of reversible data hiding in encrypted images based on most-significant-bit prediction with a very high embedding capacity. They described an efficient method (Puteaux and Puech, 2020) of noisy encrypted image correction relying on a new (cipher-feedback then electronic-code-book-mode-based) image encryption technique. Here we can use our hyperchaotic system for a new efficient encryption method as future work.

Chaotic systems include several basic properties, such as the high sensitivity to the initial conditions and system parameters, topological transitivity, non-periodicity, and pseudo-random properties (Ben Slimane et al., 2018c; Nasr et al., 2018; Devaney et al., 1993). Various chaotic systems have been developed, such as Chua circuits, Lorenz attractors and logistic maps (Wu and Baleanu, 2015; Bouallegue et al., 2011). Al-Sawalha et al. (2020) proposed an adaptive combination synchronisation of unknown chaotic Lorenz, Lü, Rössler and Chen systems. Vaidyanathan et al. (2020) designed a new multi-stable hyperjerk dynamical system with self-excited chaotic attractor, its complete synchronisation via backstepping control, circuit simulation and FPGA implementation, he also submitted a new chaotic dynamical system with a hyperbolic curve of rest points, its complete synchronisation via integral sliding mode control and circuit design (Vaidyanathan et al., 2019b). Ben Slimane et al. (2017) suggested a new behaviour of chaotic attractors with separated scrolls using the combination between the fractal process and the chaotic attractors. Bouallegue (2015b) found a method to generate a new class of chaotic attractors that possessed a multi-fractal scroll based on the fractal process. Khan and Shikha (2019) created a robust adaptive sliding mode control technique for combination synchronisation of non-identical time delay chaotic systems. However, apart from chaos' applications in various fields, it has a lot of disadvantages, especially in relation to the nature and living things (Sabir et al., 2020). Therefore, the control of such unpredictable systems has caught the attention of researcher since 1990s. Luo (2015) investigated an easy control implementation of the unpredictable behaviour of a hyperchaotic system with model uncertainties, external noise and anonymous parameters. A class of chaotic systems are characterised by the coexistence of many different types of attractors, a phenomenon referred to the multi-stability which has become a very important research topic and received much attention recently (Yu et al., 2020; Lin et al., 2020). In Signing et al. (2018), a smooth piece-wise quadratic nonlinear four-wing chaotic system is proposed. When the appropriate parameters including a two-wing and four-wing chaotic attractor are selected, the system can observe four kinds of unconnected coexisting stable states under different initial values and show rich dynamic behaviours.

Hyperchaos have more than one positive Lyapunov exponent (Bouallegue, 2015a; Ott, 2002). There are frequent similar systems such as the hyperchaotic Rössler system (Rössler, 1979; Li et al., 2005) the hyperchaotic Chua circuit and the hyperchaotic Lorenz system (Mahmoud, 2012). Li et al. (2012) introduced a hyperchaotic system using the combination between linear coupling and the systems of Mathieu and van der Pol, which were very complicated chaos behaviour having three positive Lyapunov exponents. Vaidyanathan et al. (2019a) proposed a new hyperjerk dynamical system with hyperchaotic attractor and two saddle-focus rest points exhibiting Hopf bifurcations, its hyperchaos synchronisation and circuit implementation.

It is worth knowing that neurons in the work of Bouallegue (2017) were used with only one dendrite. Various versions of neural networks have been intensively and extensively studied and successfully applied to many fields such as identifying patterns, recognising voices, controlling systems, processing signal systems, treating static images, and solving nonlinear algebraic systems (Kundu et al., 2013; Yuan and Yang, 2007; Meng and Wang, 2007; Lenze and Raddatz, 2002; Korkmaz and Kilic, 2014; Isokawa et al., 2008; Chen et al., 2014; Hsu, 2012). Our approach consists in coupling different chaotic attractors using a variable structure model of neuron (VSMN). From this structure, we give some examples of neurons with two dendrites. Then, we couple two neurons, each one with two dendrites, and the numerical simulation are done using C++ and Python. Finally, we use those neurons to couple two chaotic oscillators. Therefore, a chaotic generation by neurons with multidentrites. The numerical examples will illustrate that our multi-scroll system with hidden oscillators, symmetric, coexisting and multi-stability results is hyperchaotic.

The rest of this paper is organised as follows: in Section 2, we elaborate the new VSMN with two dendrites, their activation function, degraded activation functions and

a definition of the hidden attractors. After that we use this new neuron to generate a chaotic attractor, and we give three examples for this generation with parametric bifurcation of one of them. In Section 3, we couple two neurons each one with two dendrites with the same activation function presenting two examples, and then with different activation functions providing two examples too. In Section 4, we couple between two chaotic attractors using neurons giving an example and we find a multi-stability system. In Section 5, we conclude this paper by providing a summary of the above findings.

2 Neuron with two dendrites

In this section, we elaborate the new model of neurons presented in Bouallegue (2017), Bouallegue et al. (2020) and Nasr et al. (2020), but with two dendrites in order to increase the system's precision. The VSMN is described by the following model:

2.1 Model of neuron with two dendrites

The system is composed of two differential equations:

$$\begin{cases} \dot{u} = f_1(u, v) + X \\ \dot{v} = f_2(u, v) \end{cases} \tag{1}$$

$$\begin{cases} \dot{u} = \dfrac{-(u)}{\tau} + (u + p_1)(u + p_2) f(\beta v) f\left(\lambda (u + p_1)(u + p_2)\right) \\ + \sin(2\pi \times ft) \\ \dot{v} = -\alpha v + \chi (u + q_1)^{n_1} (u + q_2)^{n_2} \alpha f^2\left(\lambda (u + p_1)(u + p_2)\right). \end{cases} \tag{2}$$

The structure depends on seven variables n_1, n_2, p_1, p_2, q_1, q_2 and c. Moreover, u and v are the activity' states of neurons (Li and Chen, 2005). n_1, n_2, q_1 and q_2 are related to the behaviour of dendrites, p_1 and p_2 are related to the positions of dendrites, and χ represents the neuron's polarity. Furthermore, Function $f(t) = e^{-t^2/2}$, k = ±1, τ is a time constant, p and q are real numbers, and α, β and l are positive real numbers.

Figure 1 illustrates the neuron with two dendrites and its simulation using C++ program.

Figure 1 Simulation of neuron with two dendrites (see online version for colours)

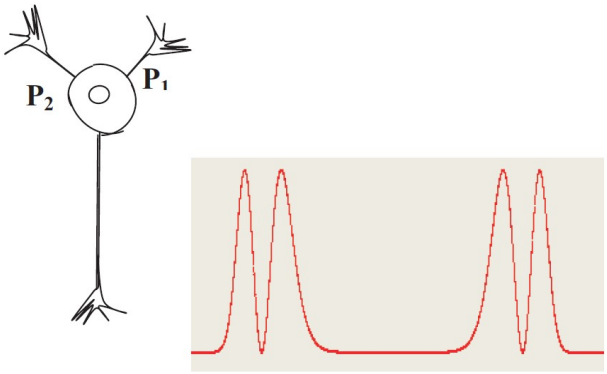

2.2 Activation function of neuron with two dendrites

The activation function of the neuron with two dendrites can be described by:

$$f(x) = (x - p_1)^{n_1} (x - p_2)^{n_2} e^{-\frac{(q_1 + x)^2 (q_2 + x)^2}{2}}. \tag{3}$$

The critical points of the function are given by equation (3.1):

$$\begin{aligned} f'(x) = & \left(n_1 (x - p_1)^{n_1 - 1} (x - p_2)^{n_2}\right. \\ & \left. + n_2 (x - p_1)^{n_1} (x - p_2)^{n_2 - 1}\right) e^{-\frac{(q_1 + x)^2 (q_2 + x)^2}{2}} \\ & - \left((q_1 + x)(q_2 + x)(x - p_1)^{n_1} (x - p_2)^{n_2} (q_1 \right. \\ & \left. + q_2 + 2x)\right) e^{-\frac{(q_1 + x)^2 (q_2 + x)^2}{2}}. \end{aligned} \tag{3.1}$$

We study the case when $n_1 = n_2 = 2$, $p_1 = -p_2$, $p_1 = q_1$ and $p_2 = q_2$. The roots of equation (3.1) are: $x_1 = 0$, $x_2 = p_1$, $x_3 = p_2$. If $p_1^4 > 2$ then $x_4 = \sqrt{p_1^2 - \sqrt{2}}$, $x_5 = -\sqrt{p_1^2 - \sqrt{2}}$, $x_6 = \sqrt{p_1^2 + \sqrt{2}}$ and $x_7 = -\sqrt{p_1^2 + \sqrt{2}}$.

In order to study the behaviour of a neuron with two dendrites influenced by a stimulator, we investigate four cases in Subsection 2.3.

2.3 Neuron model with dendrites with the same activation function

In this section, we show the results of the implementation of neuron model presented with the same activation function. Figure 2 presents the numerical simulation of VSMN with two dendrites. The two activation functions have the same value of $n_1 = n_2$ and the positions of dendrites are symmetric: $p_1 = -p_2$, $q_1 = -p_1$ and $q_2 = -p_2$.

VSMN becomes as follows:

$$\begin{cases} \dot{u} = \dfrac{-(u)}{\tau} + \left(u^2 - p_1^2\right) f(\beta v) f\left(\lambda \left(u^2 - p_1^2\right)\right) \\ + \sin(2\pi \times f \times t) \\ \dot{v} = -\alpha v + \chi \left(u^2 - q_1^2\right)^{n_1} \alpha f^2\left(\lambda \left(u^2 - p_1^2\right)\right). \end{cases} \tag{4}$$

The activation function is:

$$g(u) = \dot{v} + \alpha v = \chi \left(u^2 - q_1^2\right)^{n_1} \alpha f_2\left(\lambda \left(u^2 - p_1^2\right)\right). \tag{5}$$

To study the model, we focus on the following function:

$$g(x) = \chi \left(x^2 - q_1^2\right)^{n_1} e^{-(x^2 - p_1^2)^2/2}. \tag{6}$$

We consider $\chi = 1$. If $n \neq 0$ and $n \neq 1$, then the critical points of the function are given by:

$$\begin{aligned} & g'(x) \\ & = 2x\left(x^2 - q_1^2\right)^{n_1 - 1} \left(n_1 - \left(x^2 - q_1^2\right)\left(x^2 - p_1\right)\right) e^{-(x^2 - p_1^2)^2/2}. \end{aligned} \tag{7}$$

The roots of equation (7) are $x_1 = -q_1^2$, $x_2 = \sqrt{\frac{(p_1+q_1^2)+\sqrt{\Delta}}{2}}$, $x_3 = -\sqrt{\frac{(p_1+q_1^2)+\sqrt{\Delta}}{2}}$. If $p_1^2 > n_1$, $p_1^2 > n_1$ then $x_4 = \sqrt{\frac{(p_1+q_1^2)-\sqrt{\Delta}}{2}}$ and $x_5 = -\sqrt{\frac{(p_1+q_1^2)-\sqrt{\Delta}}{2}}$, with $\Delta = (p_1 - q_1^2)^2 = 4n_1$.

Figure 2 Behaviour of neuron with two dendrites, (a) $n_1 = 0$ and $n_2 = 0$ (b) $n_1 = 2$ and $n_2 = 2$ (c) $n_1 = 1$ and $n_2 = 1$ (d) $n_1 = 3$ and $n_2 = 3$

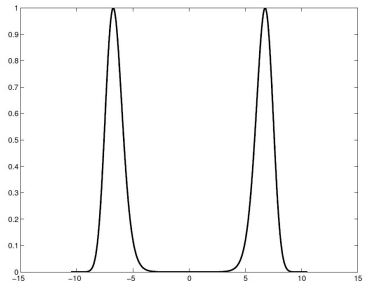

(a)

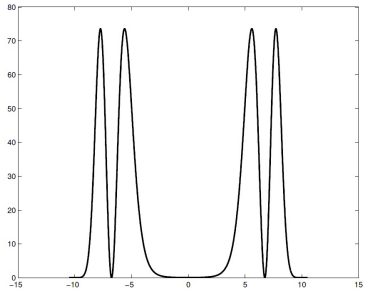

(b)

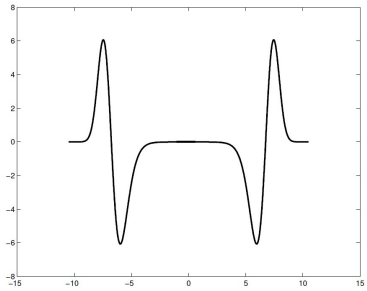

(c)

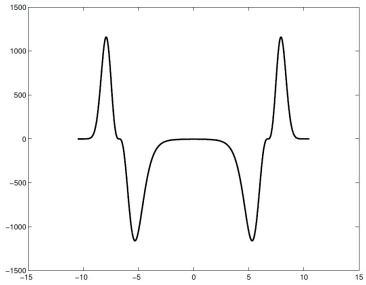

(d)

The values of the function at these critical points are $g(x_1) = 0$, $g(x_2) = (x_2^2 - q_1^2)^{n_1} e^{-(x_2^2 - p_1^2)^2/2}$, $g(x_3) = (x_3^2 - q_1^2)^{n_1} e^{-(x_3^2 - p_1^2)^2/2}$. If $g(x_4) = (x_4^2 - q_1^2)^{n_1} e^{-(x_4^2 - p_1^2)^2/2}$, and $g(x_5) = (x_5^2 - q_1^2)^{n_1} e^{-(x_5^2 - p_1^2)^2/2}$.

In order to study the behaviour of a VSMN influenced by two dendrites, we investigate four cases, with $u = f(v)$:

2.3.1 Case 1

$n_1 = n_2 = 0$, so the function becomes $g(x) = e^{-(x^2 - p_1^2)^2/2}$. Actually we have two critical points, $x_1 = -p_1$, $x_2 = p_2$ and $g(-p_1) = g(-p_2) = 1$, are the maximal function' values. Figure 2(a) is illustrated with a form that contains two lobes with the same size, one on the left and the other on the right.

2.3.2 Case 2

$n_1 = n_2 = 1$, so if $q_1 = p_1$, the function becomes $g(x) = (x^2 - p_1^2)^{n_1} e^{-(x^2 - p_1^2)^2/2}$, and the critical points are $x_1 = p_1^2 + 1$ and $x_2 = p_1^2 - 1$. The maximum value of the function is $g(x_1) = e^{-1/2}$ and the minimal' function value is $g(x_2) = -e^{-1/2}$. Figure 2(b) displays the form of the model. This form contains four lobes, every two lobes with alternate directions (up and down).

2.3.3 Case 3

$n_1 = n_2 = 2$ and $p_1 = q_1$, so the critical points are $x_1 = p_1$, $x_2 = p_1 - \sqrt{n_1}$ and $x_3 = p_1 + \sqrt{n_1}$. The values of g at these critical points are:

$$g(x_1) = 0,$$

$$g(x_2) = \left(n_1 - 2p_1\sqrt{n_1}\right)^{n_1} e^{-(n_1 + 2p_1\sqrt{n_1})^2/2},$$

$$g(x_3) = -\left(n_1 - 2p_1\sqrt{n_1}\right)^{n_1} e^{-(n_1 + 2p_1\sqrt{n_1})^2/2}.$$

If function $g(x)$ has two critical points with the same absolute maximal value, we say that the VSMN model has a stable behaviour. When the values of n are identical, the function has two maximum values:

$$g(x_2) = g(x_3)\left(n_1 - 2p_1\sqrt{n_1}\right)^{n_1} e^{-(n_1 + 2p_1\sqrt{n_1})^2/2}.$$

2.4 Degraded activation functions

In this section, we describe the normalised equations of the (VSMN). This method is used to obtain the degradation limits of the activation function in the neuron with the first and second dendrites (Bouallegue et al., 2020). From Figurw 3 we can conclude that if we add an epsilon only in the p_2 position of the second dendrite in the VSMN model, we find the degradation only on the right of the neuron. Equation (8) presents the method for the first dendrite.

$$\begin{cases} \dot{u} = \dfrac{-(u)}{\tau} + (u+p_1)(u+p_2+\varepsilon) f(\beta v) \\ f\left(\lambda(u+p_1)(u+p_2+\varepsilon)\right) + \sin(2\pi \times f \times t) \\ \dot{v} = -\alpha v + \chi (u+q_1)^{n_1} (u+q_2)^{n_2} \\ \alpha f^2 \left(\lambda(u+p_1)(u+p_2+\varepsilon)\right). \end{cases} \tag{8}$$

Figure 3 Behaviour of degraded neuron with one only dendrite (see online version for colours)

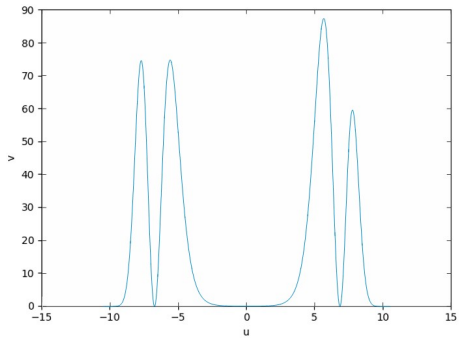

Figure 4 Behaviour of degraded neuron with two dendrites (see online version for colours)

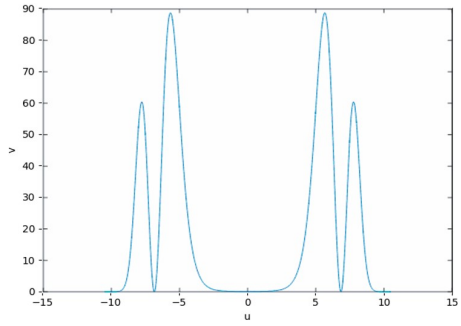

In Figure 4, note ε = 0:01, by adding just one epsilon at positions p_1 and p_2 of the dendrites in the VSMN model, we find a degradation on the right and on the left of the neuron. We notify that this degradation induces a reduction in both spikes at different positions. The system of the behaviour of the degraded neuron with two dendrites is:

$$\begin{cases} \dot{u} = \dfrac{-(u)}{\tau} + (u+p_1+\varepsilon)(u+p_2+\varepsilon) f(\beta v) \\ f\left(\lambda(u+p_1+\varepsilon)(u+p_2+\varepsilon)\right) + \sin(2\pi \times f \times t) \\ \dot{v} = -\alpha v + \chi (u+q_1)^{n_1} (u+q_2)^{n_2} \\ \alpha f^2 \left(\lambda(u+p_1+\varepsilon)(u+p_2+\varepsilon)\right). \end{cases} \tag{9}$$

2.5 *Chaotic attractors generated by neuron with two dendrites*

The movement of neurons is affected by an oscillator. Oscillations and chaos are ubiquitous phenomena that are encountered in many different areas of physics (Bouallegue, 2017). We define in this section the meaning of the hidden attractors and oscillations, and we clarify them with a generation of the oscillations of three models from the VSMN and we give a parametric bifurcation diagrams of the first example.

2.5.1 *Hidden attractors*

Recently a new concept concerning the classification of attractors has been introduced: Periodic or chaotic attractors belong either to the class of self-excited attractors or to the class of hidden attractors (Tidjani et al., 2016; Leonov et al., 2012, 2011).

The basin of attraction of a self-excited attractor overlaps with the neighbourhood of an equilibrium point, so self-excited attractors are very easy to be find. On the contrary, a hidden attractor has a basin of attraction that does not intersect with small neighbourhoods of any equilibrium points thereby making it very difficult to find; that is why one can call it hidden. Hidden attractors are important in engineering applications because they allow unexpected and potentially disastrous responses to perturbations in a structure like an aircraft control systems, drilling systems, electrical machines, and secure communications.

Leonov (2009) and Leonov et al. (2010) proposed an effective method for the numerical localisation of hidden attractors in multidimensional dynamical systems. This method was based on homotopy and numerical continuation. They constructed sequence of similar systems such that for the first system. The initial data for the numerical computation of the oscillating solution could be obtained analytically.

Then the transformation of this starting solution was tracked numerically while passing from one system to another. The first example of a hidden chaotic strange attractor was found in the Chua attractor (Leonov et al., 2012). In our case, you will find the hidden attractor in the next section.

2.5.2 *Single scroll chaotic system*

It turns out that the relationship between the behaviour of chaos and oscillations is the common factor on the parameters that depend on the mathematical model. Let us present two recurrent equations of oscillators to generate the dynamic of neuron with k_x = 1/8,000 and k_y = 1:

$$x_{n_2} = 2\cos(2\pi k_x) x_{n_1} - x_{n_0}. \tag{10}$$

The second oscillator takes the same form, its used for the second example:

$$y_{n_2} = 2\cos(2\pi k_y) y_{n_1} - y_{n_0}. \tag{11}$$

We give the first example of the new behaviour of the chaotic attractor generated by the neuron with two dendrites. The first model of the neuron with two dendrites is:

$$\begin{cases} \dot{u} = \dfrac{-(u)}{\tau} + (u+p_1)(u+p_2)\, f(\beta v) \\ f\left(\lambda(u+p_1)(u+p_2)\right) + \rho \sin(2\pi \times f \times t) \\ \dot{v} = -\alpha v + \chi (u+q_1)^{n_1} (u+q_2)^{n_2} \\ \alpha f^2 \left(\lambda(u+p_1)(u+p_2)\right). \end{cases} \tag{12}$$

Table 1 Initial conditions of single scroll chaotic system

u_0	v_0	p_1	p_2	q_1	q_2	α	β	ρ	λ
0.25	0.25	–0.8	0.6	p_1	p_2	0.1	2.667 (1 + ε)	2.5	3.75

With $n_1 = 2$, $n_2 = 2$ and the initial conditions clarified in Table 1, the new model becomes:

$$\begin{cases} \dot{u} = \dfrac{-(u)}{\tau} + (u-0.8)(u+0.6) f\left(2.667(1+\varepsilon)v\right) \\ f\left(3.75(u-0.8)(u+0.6)\right) + 2.5\sin(2\pi \times f \times t) \\ \dot{v} = -0.1v + \chi (u+p_1)^2 (u+p_2)^2\, 0.1 \\ f^2\left(3.75(u-0.8)(u+0.6)\right). \end{cases} \tag{13}$$

Figure 5 2D chaotic system from 0 to 0.8 as abscissa and from 0 to –2 as ordinate (see online version for colours)

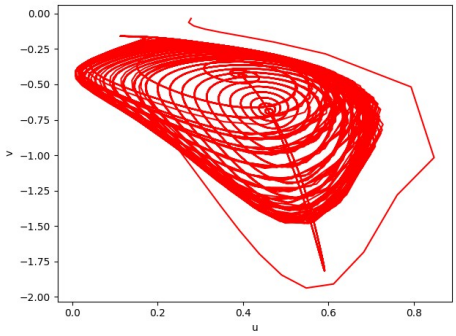

Figure 6 3D chaotic system in *u*-*v*-*w* space, from 0 to 0.8 as abscissa then from –0.3 to 0.3 as ordinate and from 0.25 to 1.75 as applicate (see online version for colours)

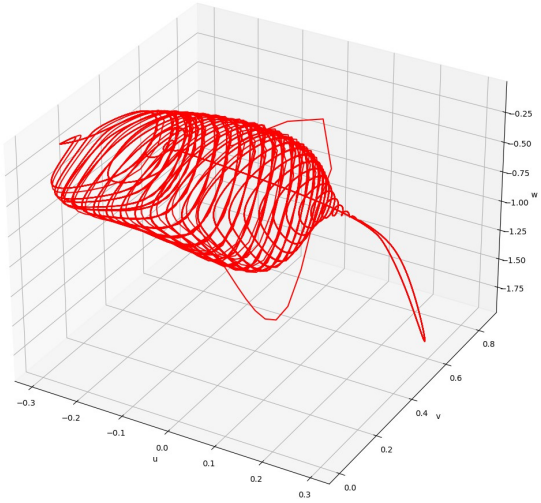

Figure 5 shows the implementation result of equation (8). Figures 5 and 6 illustrate a spiral chaotic behaviour with two orbits connected with a linear straight line. We can call them hidden chaotic attractors, too.

Figure 7 2D bifurcation diagram showing steady state behaviour of equation (13) with different gain pairs (p_1, p_2), (a) $n_1 = 0$ and $n_2 = 0$ (b) $n_1 = 2$ and $n_2 = 2$ (c) $n_1 = 1$ and $n_2 = 1$ (d) $n_1 = 3$ and $n_2 = 3$ (see online version for colours)

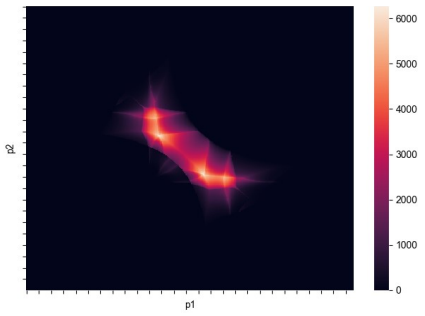

(a)

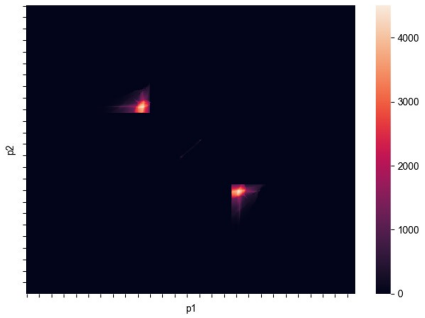

(b)

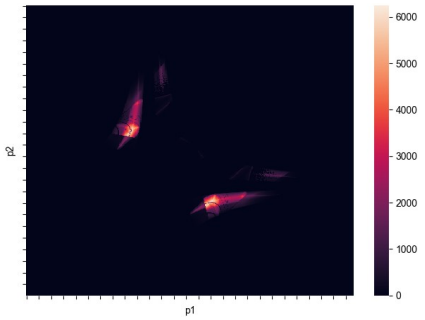

(c)

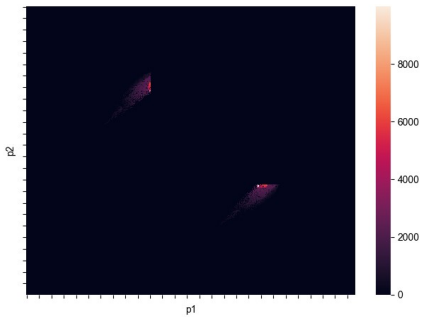

(d)

2.5.3 *Bifurcation of first example of our chaotic system*

During the last two decades, tools of analysing bifurcations and chaos have been well developed. Therefore, the investigation of the very peculiar aspect of this phenomenon has become an attractive endeavour. In this section, we analyse the time-delay influence on the stability of the steady state by taking p_1 as bifurcation parameter and fixing the value of p_2 (Li et al., 2015). The stability of equation (13) will be changed and a family of periodic orbits will bifurcate from the equilibrium with an increase of p_1.

Table 2 Four cases of the bifurcation diagrams

n_1	n_2	*Figure 7*
0	0	a
1	1	b
2	2	c
3	3	d

Four 2D bifurcation diagrams are depicted in Figure 7 and they show the steady state behaviour of equation (13) for different pairs (p_1, p_2). In addition to that, four cases are presented in Table 2. It can be easily deduced that as p_1 increases, then the first period (stable) behaviour shown in the colour orange is extended for higher values of p_1 (Miladi and Feki, 2015).

Figure 7 depicts in the colour orange the zone of the first period mode and, this matches the higher periods. Furthermore, the chaotic zones are also shown as parameters p_1 and p_2 vary (Robert et al., 2006). Particularly, when $p_1 = 0$, we observe that as p_2 raises, the output of period 6,000 becomes period 5,000. For a short interval of p_1, it becomes period 4,000 before it goes into the black period, which is the chaotic mode. We can conclude from Figure 7 that when n_1 and n_2 increase, the system takes a short periods to attack the chaotic zone.

2.5.4 *Spiral chaotic system*

The second model of neuron with two dendrites is:

$$\begin{cases} \dot{u} = f_1(u, v) + X \\ \dot{v} = f_2(u, v) + Y. \end{cases} \tag{14}$$

With $X = \rho_1 \sin(2\pi \times f \times t)$ and $Y = \rho_2 \sin(2\pi \times f \times t)$ the model become:

$$\begin{cases} \dot{u} = \dfrac{-(u)}{\tau} + (u + p_1)(u + p_2) f(\beta v) \\ f\left(\lambda (u + p_1)(u + p_2)\right) + \rho_1 \sin(2\pi \times f \times t) \\ \dot{v} = -\alpha v + \chi (u + q_1)^{n_1} (u + q_2)^{n_2} \\ \alpha f^2 \left(\lambda (u + p_1)(u + p_2)\right) + \rho_2 \sin(2\pi \times f \times t). \end{cases} \tag{15}$$

Figure 8 illustrates two scrolls in the form of two ears, connected with three curved lines to a new scroll chaotic system, where u and v are the coordinate states. We add two oscillators x_{n_2} and y_{n_2} to states u and v of our new structure, and we show that equation (15) exhibits a chaotic attractor. When we take the parameter values as $n_1 = 2$ and $n_2 = 2$ and the initial conditions presented in Table 3, with the compilation of the algorithm system, the results are in Table 3.

Table 3 Initial conditions of spiral chaotic system with two ears

u_0	v_0	p_1	p_2	q_1	q_2	α	β	ρ_1	ρ_2	λ
0.035	0.035	0.6	–0.2	0.3	p_2	0.1	2.667 $(1 + \varepsilon)$	2.5	2.5	3.75

Figure 8 Spiral chaotic system connected to two-ears attractors (see online version for colours)

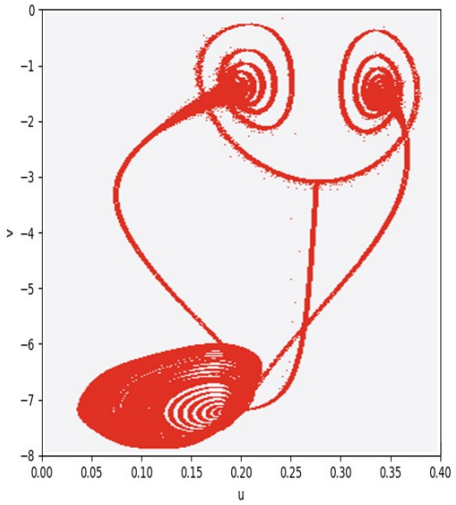

2.5.5 *Double scroll chaotic system*

The third proposed model of the neuron with two dendrites is presented in equation (17). Figure 9 shows the phase plot of the merged chaotic attractor when $\alpha = 0.1$ (we can obtain this phase plot with both $u_0 = 0.035$, $v_0 = 0.035$, …). It takes the form of a spiral chaotic attractor with two nests.

$$\begin{cases} \dot{u} = f_1(u', v') + X \\ \dot{v} = f_2(u', v') + Y. \end{cases} \tag{16}$$

The model become:

$$\begin{cases} \dot{u} = \dfrac{-(u)}{\tau} + (u + p_1)(u + p_2) f(\beta v) \\ f\left(\lambda (u + p_1)(u + p_2)\right) - \rho_1 \sin(2\pi \times f \times t) \\ \dot{v} = -\alpha v + \chi (u + q_1)^{n_1} (u + q_2)^{n_2} \\ \alpha f^2 \left(\lambda (u + p_1)(u + p_2)\right) + \rho_2 \sin(2\pi \times f \times t). \end{cases} \tag{17}$$

When $n_1 = 1$ and $n_2 = 2$, using the initial conditions in Table 4, two separated attractors become a connected one.

Therefore, the VSMN system is:

$$\begin{cases} \dot{u} = \dfrac{-(u)}{\tau} + (u+p_1)(u+p_2)\, f\left(2.667(1+\varepsilon)v\right) \\ f\left(3.75(u+0.6)(u-0.2)\right) - 2.5\sin(2\pi \times f \times t) \\ \dot{v} = -0.1v + \chi(u+p_1)^1 (u+p_2)^2\, 0.1 \\ f^2\left(3.75(u+0.6)(u-0.2)\right) + 2.5\sin(2\pi \times f \times t). \end{cases} \tag{18}$$

Table 4 Initial conditions of spiral chaotic system with two ears

u_0	v_0	p_1	p_2	q_1	q_2	α	β	ρ_1	ρ_2	λ
0.035	0.035	0.6	–0.2	0.3	p_2	0.1	2.667 (1 + ε)	2.5	2.5	3.75

Figure 9 Spiral chaotic attractor with two nests (see online version for colours)

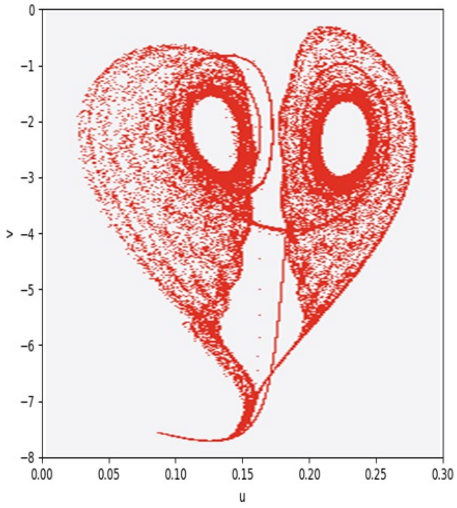

3 Coupling between two neurons having two dendrites

In this section, we give two examples for the model of neurons with two dendrites with same activation function and two examples for dendrites with different activation functions. In fact, each neuron has two dendrites.

3.1 Neurons with two dendrites with same activation function

Coupling between two different sets of neurons has been the subject of many theoretical papers over the last few years (Njitacke et al., 2020; Börgers, 2017). Despite this large amount of effort, many key issues remain open. Nonlinear dynamic system widely used to synthesise multi-scroll chaotic attractors in 2D is given. In this section, we present different cases of coupling chaotic attractors using neurons with the same activation function.

3.2 Coupling between double-scroll chaotic attractors using oscillators

In Figure 10, with the initial conditions from Table 5, that chaos can be triggered in a large parameter region. Furthermore, this portrait is plotted to illustrate the dependence of the attractor profile on the number of dendrites and the activation function. The first proposed equation is:

$$\begin{cases} \dot{u} = f_1(u,v) - X \\ \dot{v} = f_2(u,v) + Y. \end{cases} \tag{19}$$

$$\begin{cases} \dot{u}_2 = \dfrac{-\dot{u}_1}{\tau} + (u+p_1)(u+p_2)\, f(\beta v) \\ f\left(\lambda(u+p_1)(u+p_2)\right) - \rho_1 \sin(2\pi \times f \times t) \\ \dot{v}_2 = -\alpha \dot{v}_1 + \chi(u+q_1)^2 (u+q_2)^2 \\ \alpha f^2\left(\lambda(u+p_1)(u+p_2)\right) + \rho_2 \sin(2\pi \times f \times t). \end{cases} \tag{20}$$

Figure 10 illustrates a coupling chaotic behaviour with hidden attractors. They are four orbits connected with two neurons from the buttons of the first scroll to those of the second one.

Table 5 Initial conditions of coupling between two chaotic scrolls with hidden attractors

u_0	v_0	p_1	p_2	q_1	q_2	α	β	ρ_1	ρ_2	λ
0.25	–0.5	0.8	–0.6	p_1	p_2	0.1	2.667 (1 + ε)	4	14	3.75

3.2.1 Symmetric behaviour of four chaotic systems

We couple equation (22) symmetrically with a new one using two neurons, with the initial conditions of Table 6.

The system takes the following form:

$$\begin{cases} \dot{u} = f_1(u'', v'') - X \\ \dot{v} = f_2(u'', v'') + Y. \end{cases} \tag{21}$$

$$\begin{cases} \dot{u}_2 = \dfrac{-\dot{u}_1}{\tau} + (u+p_1)(u+p_2)\, f(\beta v) \\ f\left(\lambda(u+p_1)(u+p_2)\right) - \rho_1 \sin(2\pi \times f \times t) \\ \dot{v}_2 = -\alpha \dot{v}_1 + \chi(u+q_1)^2 (u+q_2)^2 \\ \alpha f^2\left(\lambda(u+p_1)(u+p_2)\right) + \rho_2 \sin(2\pi \times f \times t). \end{cases} \tag{22}$$

Figure 11 depicts two chaotic scrolls symmetrically coupled by neurons with the same chaotic scroll.

Table 6 Initial conditions of symmetric behaviour of four chaotic scrolls coupled with neurons

u_0	v_0	p_1	p_2	q_1	q_2	α	β	ρ_1	ρ_2	λ
–7	–5	–0.5	0.5	p_1	p_2	0.2	5.36067	4	14	3.75

Figure 10 Coupling between two chaotic scrolls with hidden attractors using u and v as states of the caption (see online version for colours)

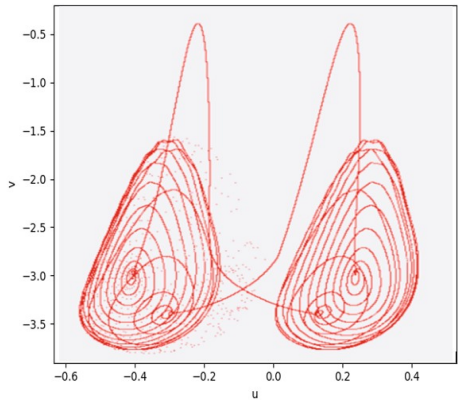

Figure 11 Symmetric behaviour of four chaotic scrolls coupled with neurons (see online version for colours)

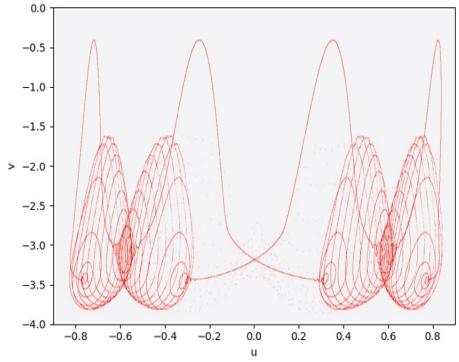

3.2.2 *Coupling between two similar chaotic attractors*

In 1988, Chua and Yang introduced the cellular neural network as a nonlinear dynamical system composed of an array of elementary and locally interacting nonlinear subsystems (Chua and Yang, 1988; Vaidyanathan, 2015). In this example, we analyse the properties of the new VSMN equation (22) and the interaction between the two spiral attractors with ears in Figure 12.

Applying equation (22), with the initial conditions of Table 7, we find the result illustrated in Figure 12.

Table 7 Initial conditions of two coexisting periodic spiral attractors with two ears

u_0	v_0	p_1	p_2	q_1	q_2	α	β	ρ_1	ρ_2	λ
0.035	0.035	1	–1	p_1	p_2	0.2	5.36067	2.5	–2.5	3.75

In Figure 12, using the curved lines in the middle of the strange chaotic attractor, we couple between two spiral chaotic systems connected with form attractors in the form of ears.

Figure 12 Two coexisting periodic spiral attractors with two ears (see online version for colours)

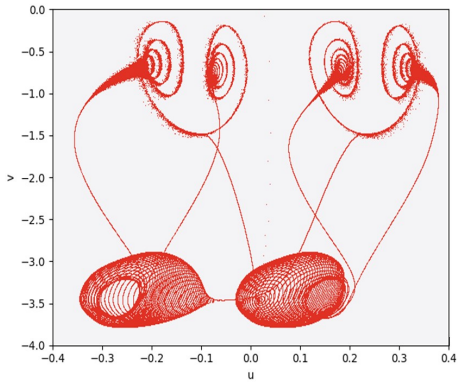

3.2.3 *Four coexisting chaotic systems*

Equation (22) provides the result illustrated in Figure 13, and the initial conditions are provided in Table 8.

In Figure 13, using the curved lines in the middle of the strange chaotic attractor, we couple between four spiral chaotic systems connected in the form of ears attractors.

Table 8 Initial conditions of four coexisting periodic spiral attractors with two ears

u_0	v_0	p_1	p_2	q_1	q_2	α	β	ρ_1	ρ_2	λ
0.35	0.35	13	–13	p_1	p_2	0.2	5.36067	2.5	–2.5	3.75

Figure 13 Four coexisting periodic spiral attractors with two ears (see online version for colours)

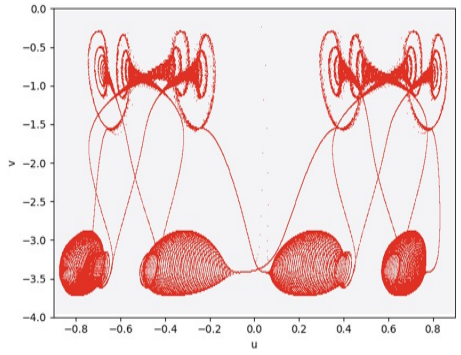

3.3 *Dendrites with different activation functions*

Producing coexisting attractors provides a new pathway for exploring the general multi-stability mechanism. Self-reproducing systems with many attractors can be constructed when a periodic function is introduced into the system and the initial conditions are used for offset control (Li et al., 2017; Li and Sprott, 2018; Li et al., 2019) where lattices of coexisting attractors are positioned in the phase space. A symmetric system hatches a symmetric pair of coexisting attractors when its symmetry is broken (Zhou et al., 2018; Lai et al., 2018). In this section, we present different examples of coexisting coupling attractors using neurons with various activation functions.

3.3.1 Coupling between double scroll chaotic systems

We couple two coexisting chaotic attractors with two nests using equation (25) and we find a new strange form of the chaotic system. With the initial conditions in Table 9, in addition to $p_1 = a_1$ and $p_2 = a_2$, the model becomes:

$$\begin{cases} \dot{u}_2 = \dfrac{-\dot{u}_1}{\tau} + (u+\alpha_1)(u+\alpha_2)\, f(\beta v) \\ f\left(\lambda(u+\alpha_1)(u+\alpha_2)\right) - \rho_1 \sin(2\pi \times f \times t) \\ \dot{v}_2 = -\alpha \dot{v}_1 + \chi (u+\alpha_1)^2 (u+\alpha_2)^2 \\ \alpha f^2 \left(\lambda(u+\alpha_1)(u+\alpha_2)\right) + \rho_2 \sin(2\pi \times f \times t). \end{cases} \tag{23}$$

Figure 14 depicts the coupling between two strange chaotic attractors with nests, with four curved lines.

Table 9 Initial conditions of two strange chaotic attractors with two merged nests

u_0	v_0	p_1	p_2	q_1	q_2	α	β	ρ_1	ρ_2	λ
0.035	0.035	1	–1	p_1	p_2	0.2	5.36067	2.5	–2.5	3.75

Figure 14 Two strange chaotic attractors with two merged nests (see online version for colours)

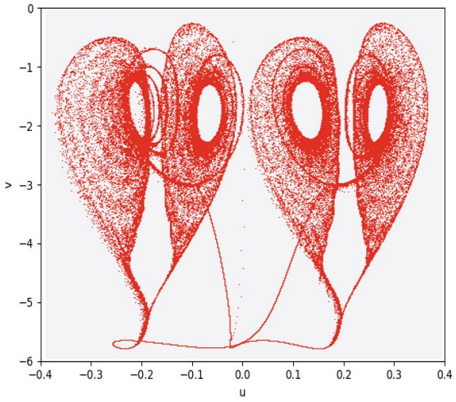

3.3.2 Coupling between chaotic systems by the same frequency

We couple four coexisting chaotic attractors with two nests using equation (26) and we find another strange form of the chaotic system.

We take the parameters in Table 10 as the initial conditions.

Table 10 Initial conditions of four strange chaotic attractors with two merged nests

u_0	v_0	p_1	p_2	q_1	q_2	α	β	ρ_1	ρ_2	λ
0.25	–0.5	12	6	0.3	p_2	0.2	5.36067	2.5	–2.5	3.75

In Figure 15, two coexisting attractors are positioned in the phase space coupled by two neurons.

Figure 15 Four strange chaotic attractors with two nests merged (see online version for colours)

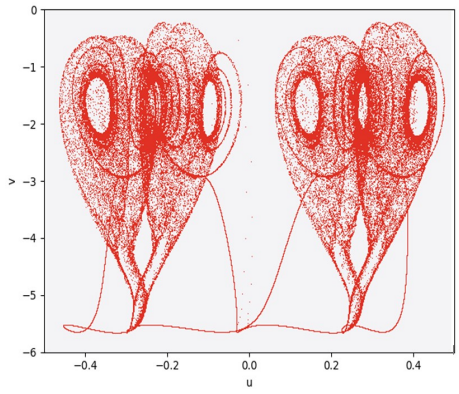

3.3.3 Coexisting of double scroll chaotic systems

We modify the sign of each position of dendrites. Figure 16 shows the same behaviour of chaotic attractors in another organisation, using the initial conditions in Table 11.

Table 11 Initial conditions of simulation of phase portrait of new chaotic system

u_0	v_0	p_1	p_2	q_1	q_2	α	β	ρ_1	ρ_2	λ
0.25	–0.5	12	12	6	p_2	0.2	5.36067	2.5	–2.5	3.75

Eight coexisting attractors are positioned Figure 16 in the phase space coupled by two neurons joined with eight curved lines.

Figure 16 Numerical simulation of phase portrait of new chaotic system (see online version for colours)

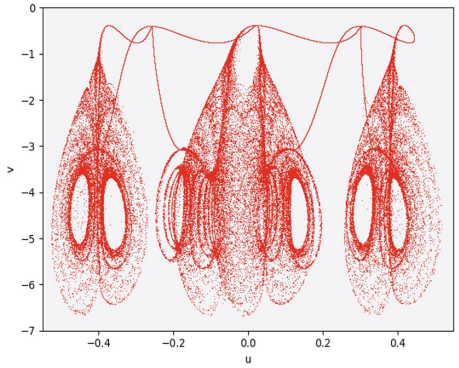

4 Multi-stability by coupling between two chaotic oscillators

It is well-known that multi-stability can lead to very complex behaviours in a dynamical system, which has been reported in some chaotic systems (Zhang et al., 2018; Li et al., 2014; Sambas et al., 2019). It is very interesting that the system can exhibit multi-stability. In this section, we present results by coupling two chaotic attractors, each one generated by a neuron with two dendrites. The VSMN model [equation (28)] and the interaction between the spiral

attractors are illustrated in Figure 17. Figure 17(a) shows the scroll chaotic attractor with two ears, and Figure 17(b) presents the same behaviour with three ears. Accordingly, strange developed attractor is plotted.

$$\begin{cases} \dot{u} = \dfrac{-(u)}{\tau} + (u+p_1)(u+p_2) f(\beta v) \\ f\left(\lambda(u+p_1)(u+p_2)\right) + \rho \dot{u}_1 \\ \dot{v}_2 = -\alpha v + \chi (u+q_1)^{n_1} (u+q_2)^{n_2} \\ \alpha f^2 \left(\lambda(u+p_1)(u+p_2)\right) - \rho \dot{v}_1. \end{cases} \tag{24}$$

We couple two chaotic attractors with neurons with multidentrites, and we find a multi-scroll system. We can conclude that the system is hyper-chaotic.

Figure 17 Coupling between two chaotic attractors with neurons having multidentrites, (a) three merged scrolls (b) four merged scrolls (see online version for colours)

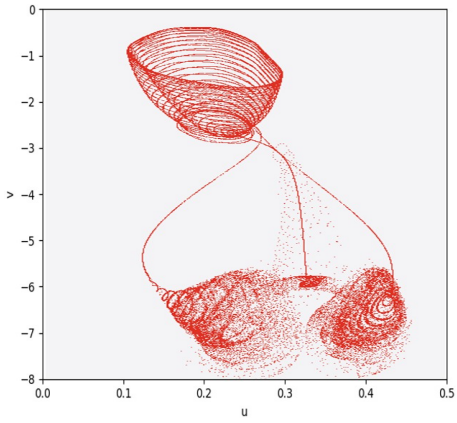

(a)

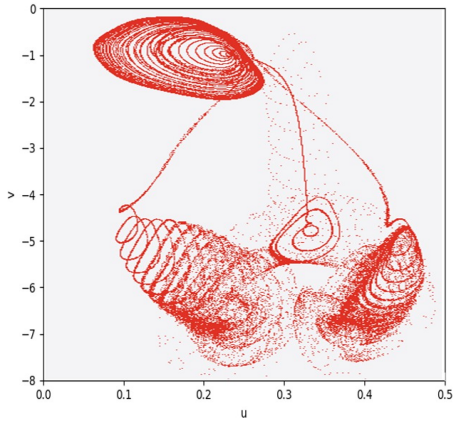

(b)

5 Conclusions

In this work we have explored various possibilities of coupling different chaotic systems using neurons. Those attractors contain separated, hidden and nested scrolls. Each scroll looks like a chaotic oscillator. The method proposed in this article put forward a new chaotic system construction and its way of generating, that's what provide new types of hyperchaotic systems. Some numerical simulation characteristics such as symmetric, coexisting and multi-stability have been provided to demonstrate that those systems are a discover of a new nonlinear chaotic system. The strong point of our new system is that it is different inside and outside from the traditional ones. That is why it will ensure a better security in the encryption or the secure communication system as future work.

References

Al-Sawalha, M.M. et al. (2020) 'Adaptive combination synchronisation of unknown chaotic Lorenz, Lü, Rössler and Chen systems', in *International Journal of Modelling, Identification and Control*, Vol. 36, No. 1, pp.34–41.

Ben Slimane, N. et al. (2018a) 'A novel chaotic image cryptosystem based on DNA sequence operations and single neuron model', in *Multimedia Tools and Applications*, Vol. 77, No. 23, pp.30993–31019.

Ben Slimane, N. et al. (2018b) 'An efficient nested chaotic image encryption algorithm based on DNA sequence', in *International Journal of Modern Physics C*, Vol. 29, No. 7, p.1850058.

Ben Slimane, N. et al. (2018c) 'Hash key-based image cryptosystem using chaotic maps and cellular automata', in *2018 15th International Multi-Conference on Systems, Signals & Devices (SSD)*, IEEE, pp.190–194.

Ben Slimane, N., Bouallegue, K. and Machhout, M. (2017) 'Designing a multi-scroll chaotic system by operating logistic map with fractal process', in *Nonlinear Dynamics*, Vol. 88, No. 3, pp.1655–1675.

Benkouider, K. et al. (2020a) 'A new family of 5D, 6D, 7D and 8D hyperchaotic systems from the 4D hyperchaotic Vaidyanathan system, the dynamic analysis of the 8D hyperchaotic system with six positive Lyapunov exponents and an application to secure communication design', in *International Journal of Modelling, Identification and Control*, Vol. 35, No. 3, pp.241–257.

Benkouider, K. et al. (2020b) 'A new family of 9D and 10D hyperchaotic systems from the 8D hyperchaotic Benkouider system, the bifurcation analysis of the 10D hyperchaotic system, circuit design and an application to secure voice communication', in *International Journal of Modelling, Identification and Control*, Vol. 36, No. 4, pp.271–289.

Börgers, C. (2017) *An Introduction to Modeling Neuronal Dynamics*, Vol. 66, Springer, Cham.

Bouallegue, G., Djemal, R. and Belwafi, K. (2020) 'Artificial EEG signal generated by a network of neurons with one and two dendrites', in *Results in Physics*, Vol. 20, p.103699, ISSN: 2211-3797.

Bouallegue, K. (2015a) 'Chaotic attractors with separated scrolls', in *Chaos: An Interdisciplinary Journal of Nonlinear Science*, Vol. 25, No. 7, p.73108.

Bouallegue, K. (2015b) 'Gallery of chaotic attractors generated by fractal network', in *International Journal of Bifurcation and Chaos*, Vol. 25, No. 1, p.1530002.

Bouallegue, K. (2017) 'A new class of neural networks and its applications', in *Neurocomputing*, Vol. 249, pp.28–47.

Bouallegue, K., Chaari, A. and Toumi, A. (2011) 'Multi-scroll and multi-wing chaotic attractor generated with Julia process fractal', in *Chaos, Solitons & Fractals*, Vol. 44, Nos. 1–3, pp.79–85.

Chen, Y., Huang, T. and Huang, Y. (2014) 'Complex dynamics of a delayed discrete neural network of two non-identical neurons', in *Chaos: An Interdisciplinary Journal of Nonlinear Science*, Vol. 24, No. 1, p.13108.

Chua, L.O. and Yang, L. (1988) 'Cellular neural networks: theory', in *IEEE Transactions on Circuits and Systems*, Vol. 35, No. 10, pp.1257–1272.

Devaney, R.L. et al. (1993) 'A first course in chaotic dynamical systems: theory and experiment', in *Computers in Physics*, Vol. 7, No. 4, pp.416–417.

Gámez-Guzmán, L. et al. (2009) 'Synchronization of Chua's circuits with multi-scroll attractors: application to communication', in *Communications in Nonlinear Science and Numerical Simulation*, Vol. 14, No. 6, pp.2765–2775.

Hsu, W-Y. (2012) 'Application of competitive Hopfield neural network to brain-computer interface systems', in *International Journal of Neural Systems*, Vol. 22, No. 1, pp.51–62.

Isokawa, T. et al. (2008) 'Associative memory in quaternionic Hopfield neural network', in *International Journal of Neural Systems*, Vol. 18, No. 2, pp.135–145.

Khan, A. and Shikha (2019) 'Robust adaptive sliding mode control technique for combination synchronisation of non-identical time delay chaotic systems', in *International Journal of Modelling, Identification and Control*, Vol. 31, No. 3, pp.268–277.

Korkmaz, N. and Kilic, R. (2014) 'Implementations of modified chaotic neural models with analog reconfigurable hardware', in *International Journal of Bifurcation and Chaos*, Vol. 24, No. 4, p.1450046.

Kundu, A., Das, P. and Roy, A.B. (2013) 'Complex dynamics of a four neuron network model having a pair of short-cut connections with multiple delays', in *Nonlinear Dynamics*, Vol. 72, No. 3, pp.643–662.

Lai, Q. et al. (2018) 'Coexisting attractors and circuit implementation of a new 4D chaotic system with two equilibria', in *Chaos, Solitons & Fractals*, Vol. 107, pp.92–102, ISSN: 0925-2312.

Lenze, B. and Raddatz, J. (2002) 'Effects of dilation and translation on a perceptron-type learning rule for higher order Hopfield neural networks', in *International Journal of Neural Systems*, Vol. 12, No. 2, pp.83–93.

Leonov, G.A. (2009) 'On the method of harmonic linearization', in *Automation and Remote Control*, Vol. 70, No. 5, pp.800–810.

Leonov, G.A., Kuznetsov, N.V. and Vagaitsev, V.I. (2011) 'Localization of hidden Chuas attractors', in *Physics Letters A*, Vol. 375, No. 23, pp.2230–2233.

Leonov, G.A., Kuznetsov, N.V. and Vagaitsev, V.I. (2012) 'Hidden attractor in smooth Chua systems', in *Physica D: Nonlinear Phenomena*, Vol. 241, No. 18, pp.1482–1486.

Leonov, G.A., Vagaitsev, V.I. and Kuznetsov, N.V. (2010) 'Algorithm for localizing Chua attractors based on the harmonic linearization method', in *Doklady Mathematics*, Vol. 82, No. 1, pp.663–666.

Li, C. and Chen, G. (2005) 'Coexisting chaotic attractors in a single neuron model with adapting feedback synapse', in *Chaos, Solitons & Fractals*, Vol. 23, No. 5, pp.1599–1604.

Li, C. and Sprott, J.C. (2018) 'An infinite 3-D quasiperiodic lattice of chaotic attractors', in *Physics Letters A*, Vol. 382, No. 8, pp.581–587.

Li, C. et al. (2019) 'Doubling the coexisting attractors', in *Chaos: An Interdisciplinary Journal of Nonlinear Science*, Vol. 29, No. 5, p.51102.

Li, C., Sprott, J.C. and Mei, Y. (2017) 'An infinite 2-D lattice of strange attractors', in *Nonlinear Dynamics*, Vol. 89, No. 4, pp.2629–2639.

Li, C., Sprott, J.C. and Thio, W. (2014) 'Bistability in a hyperchaotic system with a line equilibrium', in *Journal of Experimental and Theoretical Physics*, Vol. 118, No. 3, pp.494–500.

Li, N., Tan, W. and Zhao, H. (2015) 'Hopf bifurcation analysis and chaos control of a chaotic system without Ilnikov orbits', in *Discrete Dynamics in Nature and Society*, Vol. 2015, No. 1026-0226, 10pp.

Li, Q., Yang, X-S. and Yang, F. (2005) 'Hyperchaos in Hopfield-type neural networks', in *Neurocomputing*, Vol. 67, pp.275–280, ISSN: 0925-2312.

Li, S-Y. et al. (2012) 'Generating tri-chaos attractors with three positive Lyapunov exponents in new four order system via linear coupling', in *Nonlinear Dynamics*, Vol. 69, No. 3, pp.805–816.

Lin, H. et al. (2020) 'Firing multistability in a locally active memristive neuron model', in *Nonlinear Dynamics*, Vol. 100, No. 4, pp.3667–3683.

Luo, R. (2015) 'The robust adaptive control of chaotic systems with unknown parameters and external disturbance via a scalar input', in *International Journal of Adaptive Control and Signal Processing*, Vol. 29, No. 10, pp.1296–1307.

Mahmoud, E.E. (2012) 'Dynamics and synchronization of new hyperchaotic complex Lorenz system', in *Mathematical and Computer Modelling*, Vol. 55, Nos. 7–8, pp.1951–1962.

Meng, J. and Wang, X-y. (2007) 'Robust antisynchronization of a class of delayed chaotic neural networks', in *Chaos: An Interdisciplinary Journal of Nonlinear Science*, Vol. 17, No. 2, p.23113.

Miladi, Y. and Feki, M. (2015) 'Bifurcation, quasiperiodicity, chaos, and co-existence of different behaviors in the controlled H-bridge inverter', in *Handbook of Research on Advanced Intelligent Control Engineering and Automation*, pp.301–332, IGI Global publisher of Timely Knowledge.

Nasr, S., Bouallegue, K. and Mekki, H. (2020) 'Fractal, chaos and neural networks in path generation of mobile robot', in *International Journal of Modelling, Identification and Control*, Vol. 34, No. 1, pp.41–50.

Nasr, S., Mekki, H. and Bouallegue, K. (2019) 'A multi-scroll chaotic system for a higher coverage path planning of a mobile robot using flatness controller', in *Chaos, Solitons & Fractals*, Vol. 118, pp.366–375, ISSN: 0960-0779.

Njitacke, Z.T. et al. (2020) 'Coexistence of firing patterns and its control in two neurons coupled through an asymmetric electrical synapse', in *Chaos: An Interdisciplinary Journal of Nonlinear Science*, Vol. 30, No. 2, p.23101.

Ott, E. (2002) *Chaos in Dynamical Systems*, Cambridge University Press, Cambridge Core.

Puteaux, P. and Puech, W. (2017) 'Reversible data hiding in encrypted images based on adaptive local entropy analysis', in *2017 Seventh International Conference on Image Processing Theory, Tools and Applications (IPTA)*, IEEE, pp.1–6.

Puteaux, P. and Puech, W. (2018) 'An efficient MSB prediction-based method for high-capacity reversible data hiding in encrypted images', in *IEEE Transactions on Information Forensics and Security*, Vol. 13, No. 7, pp.1670–1681.

Puteaux, P. and Puech, W. (2020) 'CFB-then – ECB mode-based image encryption for an efficient correction of noisy encrypted images', in *IEEE Transactions on Circuits and Systems for Video Technology*, Vol. 31, No. 9, pp.3338–3351.

Robert, B., Feki, M. and Iu, H.H.C. (2006) 'Control of a PWM inverter using proportional plus extended time-delayed feedback', in *International Journal of Bifurcation and Chaos*, Vol. 16, No. 1, pp.113–128.

Rössler, O.E. (1979) 'An equation for hyperchaos', in *Physics Letters A*, Vol. 71, Nos. 2–3, pp.155–157.

Sabir, M. et al. (2020) 'Observer and descriptor satisfying incremental quadratic constraint for class of chaotic systems and its applications in a quadrotor chaotic system', in *Chaos, Solitons & Fractals*, Vol. 137, p.109874, ISSN: 0960-0779.

Sambas, A. et al. (2019) 'Multistability in a novel chaotic system with perpendicular lines of equilibrium: analysis, adaptive synchronization and circuit design', in *Engineering Letters*, Vol. 27, No. 4, p.12.

Signing, V.R.F., Kengne, J. and Kana, L.K. (2018) 'Dynamic analysis and multistability of a novel fourwing chaotic system with smooth piecewise quadratic nonlinearity', in *Chaos, Solitons & Fractals*, Vol. 113, pp.263–274, ISSN: 0960-0779.

Tidjani, M., Lozi, R. and Chua, L. (2016) 'Hidden bifurcation in the multispiral chua attractor', in *International Journal of Bifurcation and Chaos in Applied Sciences and Engineering*, Vol. 26, No. 14, p.1630039-1.

Trejo-Guerra, R. et al. (2009) 'Chaotic communication system using Chua's oscillators realized with CCII+ s', in *International Journal of Bifurcation and Chaos*, Vol. 19, No. 12, pp.4217–4226.

Vaidyanathan, S. (2015) 'Hybrid chaos synchronization of 3-cells cellular neural network attractors via adaptive control method', in *International Journal of PharmTech Research*, Vol. 8, No. 8, pp.61–73.

Vaidyanathan, S., Moroz, I.M. and Sambas, A. (2019a) 'A new hyperjerk dynamical system with hyperchaotic attractor and two saddle-focus rest points exhibiting Hopf bifurcations, its hyperchaos synchronisation and circuit implementation', in *International Journal of Modelling, Identification and Control*, Vol. 33, No. 4, pp.299–310.

Vaidyanathan, S. et al. (2019b) 'A new chaotic dynamical system with a hyperbolic curve of rest points, its complete synchronisation via integral sliding mode control and circuit design', in *International Journal of Modelling, Identification and Control*, Vol. 33, No. 3, pp.198–207.

Vaidyanathan, S. et al. (2020) 'A new multistable hyperjerk dynamical system with self-excited chaotic attractor, its complete synchronisation via backstepping control, circuit simulation and FPGA implementation', in *International Journal of Modelling, Identification and Control*, Vol. 35, No. 3, pp.177–190.

Wu, G-C. and Baleanu, D. (2015) 'Discrete chaos in fractional delayed logistic maps', in *Nonlinear Dynamics*, Vol. 80, No. 4, pp.1697–1703.

Yu, F. et al. (2020) 'Multistability analysis, coexisting multiple attractors, and FPGA implementation of Yu-Wang four-wing chaotic system', in *Mathematical Problems in Engineering* Vol. 2020, No. 7530976, 16pp.

Yuan, Q. and Yang, X-S. (2007) 'Computer assisted verification of chaos in three-neuron cellular neural networks', in *International Journal of Bifurcation and Chaos*, Vol. 17, No. 12, pp.4381–4386.

Zhang, S. et al. (2018) 'Generating one to four-wing hidden attractors in a novel 4D no-equilibrium chaotic system with extreme multistability', in *Chaos: An Interdisciplinary Journal of Nonlinear Science*, Vol. 28, No. 1, p.13113.

Zhou, L., Wang, C. and Zhou, L. (2018) 'A novel no-equilibrium hyperchaotic multi-wing system via introducing memristor', in *International Journal of Circuit Theory and Applications*, Vol. 46, No. 1, pp.84–98.